Tunable Light Emission from GaN-Based Photonic Crystal with Ultraviolet AlN/AlGaN Distributed Bragg Reflector

2011 Jpn. J. Appl. Phys. 50 04DG09

(http://iopscience.iop.org/1347-4065/50/4S/04DG09)

DOI: 10.1143/JJAP.50.04DG09

Tunable Light Emission from GaN-Based Photonic Crystal with Ultraviolet AlN/AlGaN Distributed Bragg Reflector

Cheng-Chang Chen[1], Ching-Hsueh Chiu[1], Yi-Chun Yang[2], M. H. Shih[1,2*], Jun-Rong Chen[1], Zhen-Zu Li[1], Hao-Chung Kuo[1], and Tien-Chang Lu[1]

[1] *Department of Photonics and Institute of Electro-Optical Engineering, National Chiao Tung University, Hsinchu 30010, Taiwan, R.O.C.*
[2] *Research Center for Applied Sciences (RCAS), Academia Sinica, Nankang, Taipei 115, Taiwan, R.O.C.*

Received September 21, 2010; accepted December 8, 2010; published online April 20, 2011

In this paper, the characteristics of GaN-based two-dimensional (2D) photonic crystal bandedge coupling operation with an ultraviolet AlN/AlGaN distributed Bragg reflector (DBR) have been investigated and analyzed. The 25-pair $AlN/Al_{0.2}GaN_{0.8}$ DBR shows a high reflectivity of 85% at 375 nm with the stop-band width of 15 nm. A strong light emission was observed from GaN photonic crystals within high reflectivity region of DBR. The emission wavelength can be also manipulated by varying the radius to lattice constant ratio. The photonic crystal bandedge mode was also characterized with three-dimensional plane-wave expansion (PWE) and finite-difference time-domain (FDTD) simulation.

1. Introduction

Recently, GaN-based materials have been a great deal of attention due to the large direct band gap and the promising potential for the optoelectronic devices, including light emitting diodes (LED), laser diodes (LD),[1–5] display, storage, and illumination. High reflectivity nitride-based distributed Bragg reflectors (DBR) are important for the development of GaN-based optical devices such as resonant-cavity light-emitting diodes (RCLEDs)[6] and vertical-cavity surface-emitting lasers (VCSEL).[7,8] In particular, a small optical mode volume can emit a single longitudinal mode with a symmetrically circular beam and a small beam divergence that are superior to the edge emitting lasers and desirable for many practical applications in high density optical storage, and laser printing. Today, wide-bandgap III–nitride-based LEDs has been used as flashlight and lighting to replace the traditional lighting sources due to its higher efficiency. The blue LD can serve as the light source for high density storage system because of its short wavelength. Therefore the high efficiency and the short wavelength of GaN-based light sources are on-demand for many applications.

In the meantime, photonic crystals (PC) possess many advantages for controlling light emission and propagation, and have been applied for new optical devices.[9–11] In general, there are two main methods to improve light extraction by mean of PC structure. One is the use of the photonic band gap (PBG) to inhibit the propagation of guided modes;[12] the other is utilizing PC structure to couple guided modes to radiative modes.[13–17] The GaN-based PC light emitters had been studied for blue wavelengths,[17–20] and several structures had included PCs and blue wavelengths distributed Bragg reflector (DBR)[20] for better vertical confinement. However further studies in ultraviolet (UV) emission from GaN PCs with UV DBR have not been reported. In this paper, we demonstrated room temperature UV light enhancement from GaN-based two-dimensional (2D) PCs with bottom AlN/AlGaN DBR. The emission wavelength was also manipulated by controlling the ratio of r/a (radius over lattice constant) of PC lattices. The DBR structure has center stop-band at 375 nm and a width approximately 15 nm. Therefore, it can be acted as a mirror to reflect light from the bottom area and played the role as a lower refracted index layer to control the guided modes.

2. Fabrication Process

The 2D photonic crystal square lattices were fabricated in an ultraviolet AlN/AlGaN distributed Bragg reflector (UV DBR) structure. This DBR structure was grown by a low pressure metal–organic chemical vapor deposition (MOCVD) system on a (0001)-oriented sapphire substrates. A 2-μm-thick undoped GaN was first grown on a *C*-plane (0001) sapphire substrate. Then 25-pair $AlN/Al_{0.2}Ga_{0.8}N$ structure was grown at 900 °C, followed by a 200 nm undoped GaN gain layer on the top of the epitaxial structure. The schematic structure of the wafer is shown in Fig. 1(a), and the cross-section scanning electron microscopy (SEM) image of the wafer structure is shown in Fig. 1(b). The structural quality of the UV DBR layers is maintained by compensating the compressive and tensile stress in each $\lambda/4$ pair. This approach results in the lowest elastic strain energy and allows the growth of thick coherently strained DBR. The growth details were reported in our previous works.[21,22)]

To fabricate the PC lattices, a 300 nm Si_3N_4 layer and a 300 nm poly(methyl methacrylate) (PMMA) layer were deposited as the masks during the process. According to the simulation of plane-wave expansion (PWE),[23–25] we can design and utilize PC structures to inhibit emission of guided modes or redirect trapped light into radiated modes. The PC square lattice patterns were defined on the PMMA layer by E-beam lithography and the patterns were transferred into Si_3N_4 layer in reactive ion etching (RIE) with CHF_3/O_2 mixture. The structure was then etched by inductively coupled plasma (ICP) RIE (ICP-RIE) with Cl_2/Ar mixture. The mask layers were removed at the end of processes. The size of a fabricated photonic crystal pattern is approximately $50 \times 50\,\mu m^2$ with a lattice constant (a) of 250 nm and a hole radius of 0.28a. The etch depth of the holes is approximately 500 nm which is pass through undoped GaN layer into DBR region. The schematic structure of the fabricated PCs in AlN/AlGaN DBR is shown in Fig. 2(a). The top view of a SEM image of a fabricated PC pattern on the GaN-based structure is shown in Fig. 2(b).

*E-mail address: mhshih@gate.sinica.edu.tw

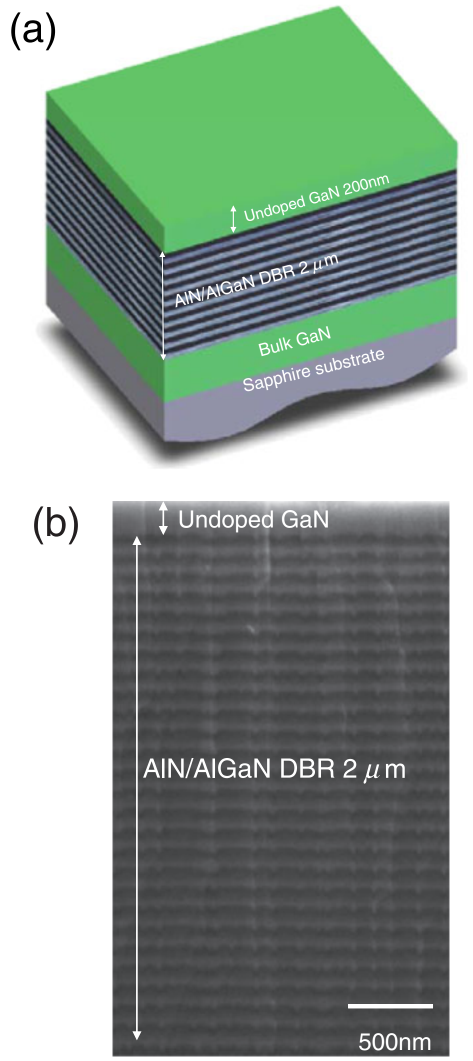

Fig. 1. (Color online) (a) Schematic structure of the epitaxial layers. The ultraviolet AlN/AlGaN distributed Bragg reflector contains 25 periods of $\lambda/4$ pairs. (b) The SEM image of the epitaxial gain layer with DBR structure from cross-section view.

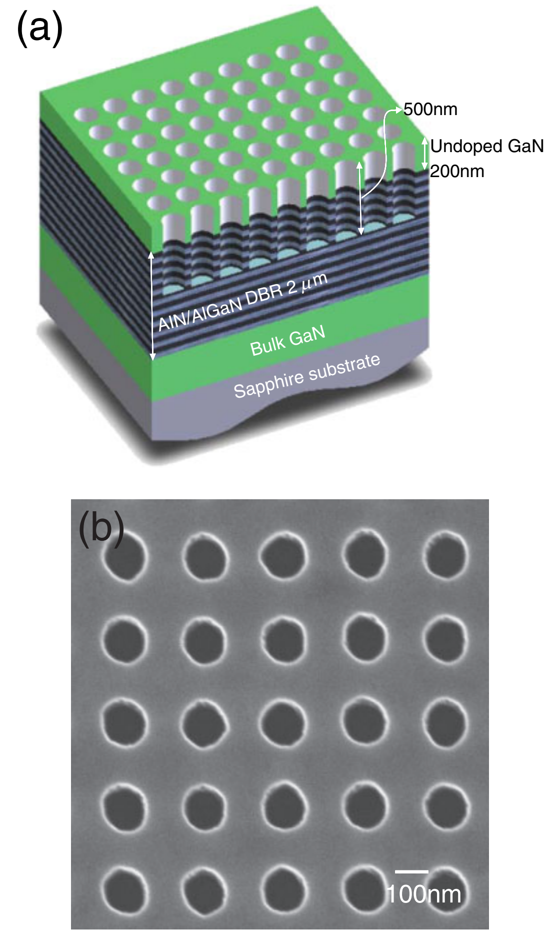

Fig. 2. (Color online) (a) Schematic structure of the square PC patterns with a depth 500 nm and total square area of a width about 50 μm. (b) The top view SEM image of the photonic crystal square lattices.

3. Measurement and Discussion

Before characterizing the PC with the AlN/AlGaN DBR structure, the high reflectivity in UV region from the DBR layers was characterized. The UV DBR structure is designed for the UV wavelength around 360 nm. The thicknesses of AlN and AlGaN layers are 45 and 42 nm can be expressed by

$$d_{\mathrm{AlN}} = \frac{\lambda}{4n_{\mathrm{AlN}}} \quad \text{and} \quad d_{\mathrm{AlGaN}} = \frac{\lambda}{4n_{\mathrm{AlGaN}}},$$

where n_{AlN} and n_{AlGaN} are refractive indices of AlN and AlGaN which are 2.03 and 2.19, respectively. The blue-dotted curve in Fig. 3(a) is the measured spectrum by an optical constant UV–visible spectrometer with a normal incident light from 300 to 440 nm wavelength. The UV DBR has the highest reflectivity of 85% at the center wavelength of 375 nm, with a stop-band width of about 15 nm. To demonstrate the light enhancement from the PC structure, the optical pumping was performed by using a frequency-tripled Nd:YVO_4 355 nm pulsed laser with a pulse width of 500 ps and a repetition rate of 1 kHz. The device was pumped by a normal incident laser beam with a spot size of 50 μm which can cover the whole PC pattern area. The light emission from the sample was collected by a 15× objective lens through a multi-mode fiber, and coupled into a spectrometer with a charge coupled device detectors.

Figure 3(a) shows the measured spectra from the photonic crystal DBR structure (black curve) and non-patterned region (red curve). A strong light emission from the photonic crystal pattern was observed. The resonant peak was observed at 374 nm wavelength. A 5-fold enhancement in photoluminescence emission was also achieved, compared with the emission from the unpatterned area on the same sample as shown in Fig. 3(a). It was worth to be noted that the output intensity is in the stop-band width of DBR, which could be due to that the bottom DBR can be treated as a high reflectivity reflector mirror, benefiting emission efficiency. Figure 3(b) shows the measured polarization curve of the light emission. This UV emission does not have a definite polarization direction, and has a low degree of polarization of 11%. This result indicates the bandedge mode operation, which oscillates along several in-plane directions.

One of the advantages of photonic crystal lasers is their resonant wavelength can be manipulated by the geometrical parameters. Here, we demonstrated resonant wavelength

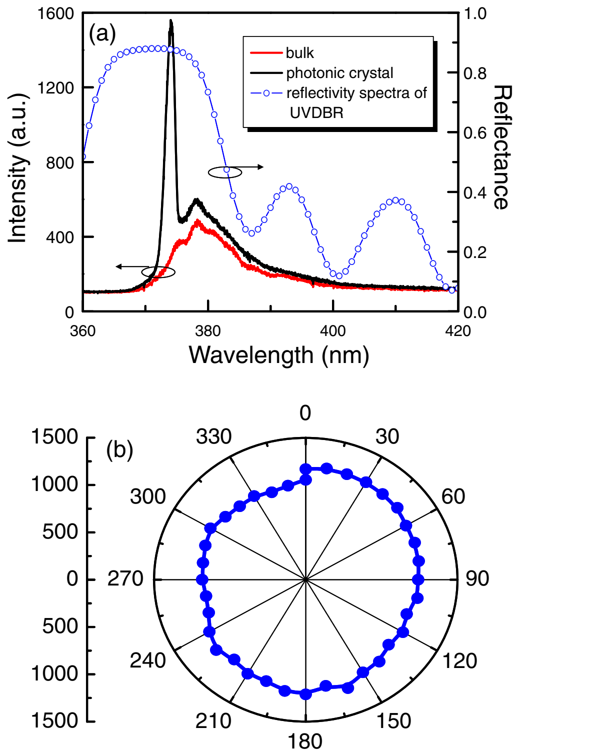

Fig. 3. (Color online) (a) Measured reflectivity spectrum (blue-dotted curve) of the AlN/AlGaN DBR structure and photoluminescence spectra of unpatterned (red curve) and patterned (black curve) UV DBR structure at room temperature. This peak wavelength is 374 nm which is inside stop-band of DBR. (b) Polarization curve of the light emission from the GaN-based PCs.

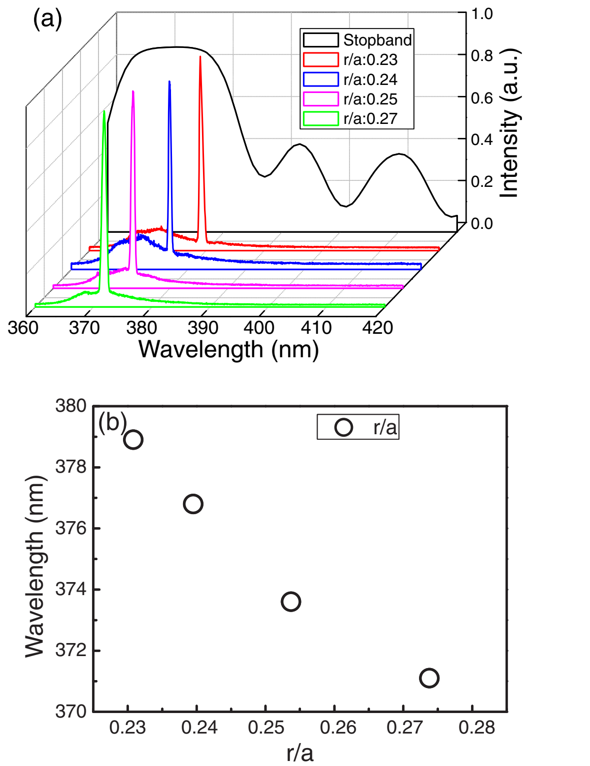

Fig. 4. (Color online) (a) The emission spectra from GaN-based photonic crystals with different of r/a values. (b) The resonant wavelength versus r/a value of photonic crystal lattices.

tuning of the UV GaN-based PCs by varying hole radius to lattice constant ratio (r/a). Figure 4(a) shows the emission spectra from GaN photonic crystals with the different of r/a values of 0.27, 0.25, 0.24, and 0.23. The wavelengths of resonant peaks with different r/a values were also recorded in Fig. 4(b). The resonant wavelengths of spectra are 371.1, 373.6, 376.8, and 378.6 nm, which are located within the stop-band width of GaN DBR. Therefore the tunable UV emission within the high reflection region of GaN DBR can be expected by tuning of r/a value of the structure.

4. Simulation and Analysis

In order to understand optical modes of the GaN-based PC structure, plane-wave expansion (PWE) method and finite-difference time-domain (FDTD) were used to perform the simulations. Figure 5(a) shows calculated band diagram of the GaN PCs from PWE method between normalized frequency (a/λ) 0.6 and 0.8. The red region in Fig. 5(a) indicates the high reflection region due to the UV GaN-based DBR at the bottom of PC lattices. Because the photonic band is almost flat and the group velocity approaches zero at PC band edge, the strong resonances at the specific frequencies are expected to be observed in the experiment. In measured results, the strong resonance at 374 nm wavelength was observed from the PC structure with 250 nm lattice constant. This optical mode, which is corresponded to a normalized frequency of $a/\lambda = 0.66$, is bandedge emission at the symmetry point Γ in the band diagram.

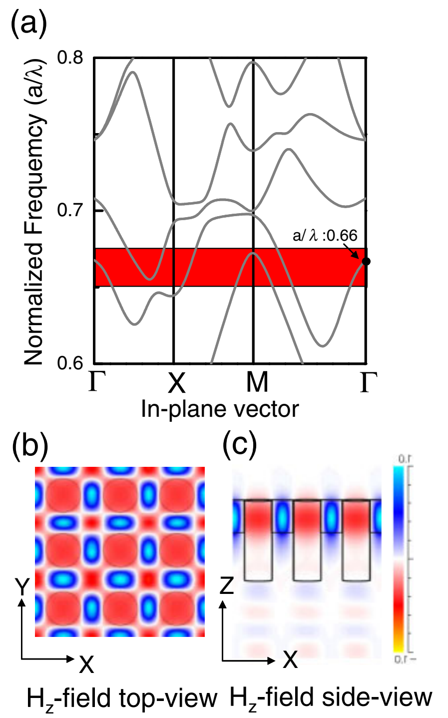

Fig. 5. (Color online) (a) The corresponding band diagram calculated by the PWE method. The calculated H_z field by FDTD simulation from (b) top view and (c) cross-section view.

Figure 5(b) shows the calculated in-plane H_z field profile of the operated mode from FDTD simulation. This in-plane mode profile also confirms mode behavior of the bandedge mode at the Γ point. Figure 5(c) is the vertical H_z field profile of the operated mode along the *x*-axis. According to the vertical mode profile, the optical mode is clearly located in the 200 nm un-doped GaN layer due to the high reflection of the UV DBR. The UV DBR plays an important role to select emission wavelength in the GaN-based PC structure. The gain peak of the GaN without the DBR is around 360 nm wavelength. However, the observed resonant modes are around 374 nm wavelength. There is a 14 nm wavelength difference between GaN gain peak and the resonant mode. It is attributed to the reflection of the UV DBR mirror on the bottom of PC lattices. This DBR effect in the GaN expitaxial structure had been observed in our previous works.[22,26]

5. Conclusions

In short, the UV light enhancement from the GaN-based PCs with AlN/AlGaN DBR is achieved. Tunable light emissions were demonstrated by varying the r/a value of PC lattices. This enhancement results from the coupling between emission in the top GaN gain layer and a bandedge mode at symmetry point Γ. The optical mode profile of this symmetric bandedge mode was also characterized with PWE and FDTD simulation. Due to the larger enhancement of the devices, the PC structure with bottom DBR mirror could be one of potential UV light sources for the future applications.

Acknowledgment

The authors are also grateful to the National Chiao Tung University's Center for Nano Science and Technology and the National Science Council of the Republic of China, Taiwan, for financially supporting this research under contract no. NSC 98-3114-E009-CC2, and NSC 99-2112-M-001-033-MY3.

1) S. Nakamura, M. Senoh, N. Iwasa, and S. Nagahama: Jpn. J. Appl. Phys. **34** (1995) L797.
2) S. Nakamura, T. Mukai, and M. Senoh: Appl. Phys. Lett. **64** (1994) 1687.
3) S. Nakamura, S. Pearton, and G. Fasol: *The Blue Laser Diode: The Complete Story* (Springer, Berlin, 2000).
4) E. D. Haberer, R. Sharma, C. Meier, A. R. Stonas, S. Nakamura, S. P. DenBaars, and E. L. Hu: Appl. Phys. Lett. **85** (2004) 5179.
5) A. C. Tamboli, E. D. Haberer, R. Sharma, K. H. Lee, S. Nakamura, and E. L. Hu: Nat. Photonics **1** (2006) 61.
6) M. Diagne, Y. He, H. Zhou, E. Makarona, A. V. Nurmikko, J. Han, K. E. Waldrip, J. J. Figiel, T. Takeuchi, and M. Krames: Appl. Phys. Lett. **79** (2001) 3720.
7) T. C. Lu, S. W. Chen, L. F. Lin, T. T. Kao, C. C. Kao, P. Yu, H. C. Kuo, S. C. Wang, and S. Fan: Appl. Phys. Lett. **92** (2008) 011129.
8) T. C. Lu, C. C. Kao, H. C. Kuo, G. S. Huang, and S. C. Wang: Appl. Phys. Lett. **92** (2008) 141102.
9) E. Yablonovitch: Phys. Rev. Lett. **58** (1987) 2059.
10) S. John: Phys. Rev. Lett. **58** (1987) 2486.
11) J. D. Joannopoulos, P. R. Villeneuve, and S. Fan: Nature (London) **386** (1997) 143.
12) M. Boroditsky, T. F. Krauss, R. Coccioli, R. Vrijen, R. Bhat, and E. Yablonovitch: Appl. Phys. Lett. **75** (1999) 1036.
13) N. Eriksson, M. Hagberg, and A. Larsson: IEEE J. Quantum Electron. **32** (1996) 1038.
14) A. L. Fehrembach, S. Enoch, and A. Sentenac: Appl. Phys. Lett. **79** (2001) 4280.
15) M. Rattier, H. Benisty, E. Schwoob, C. Weisbuch, T. F. Krauss, C. J. M. Smith, R. Houdre, and U. Oesterle: Appl. Phys. Lett. **83** (2003) 1283.
16) D. Delbeke, P. Bienstman, R. Bockstaele, and R. Baets: J. Opt. Soc. Am. B **19** (2002) 871.
17) A. David, T. Fujii, R. Sharma, K. McGroddy, S. Nakamura, S. P. DenBaars, E. L. Hu, C. Weisbuch, and H. Benisty: Appl. Phys. Lett. **88** (2006) 061124.
18) H. Matsubara, S. Yoshimoto, H. Saito, Y. Jianglin, Y. Tanaka, and S. Noda: Sciences **319** (2008) 445.
19) D. H. Kim, C. O. Cho, Y. G. Roh, H. Jeon, Y. S. Park, J. Cho, J. S. Im, C. Sone, Y. Park, W. J. Choi, and Q. H. Park: Appl. Phys. Lett. **87** (2005) 203508.
20) T. C. Lu, S. W. Chen, T. T. Kao, and T. W. Liu: Appl. Phys. Lett. **93** (2008) 111111.
21) G. S. Huang, T. C. Lu, H. H. Yao, H. C. Kuo, S. C. Wang, C. W. Lin, and L. Chang: Appl. Phys. Lett. **88** (2006) 061904.
22) J. R. Chen, S. C. Ling, C. T. Hung, T. S. Ko, T. C. Lu, H. C. Kuo, and S. C. Wang: J. Cryst. Growth **310** (2008) 4871.
23) E. Yablonobitch, T. J. Gmitter, and R. Bhat: Phys. Rev. Lett. **61** (1987) 2546.
24) S. Fan, P. R. Villeneuve, J. D. Joannopoulos, and E. F. Schubert: Phys. Rev. Lett. **78** (1997) 3294.
25) M. Plihal and A. A. Maradudin: Phys. Rev. B **44** (1991) 8565.
26) C. C. Chen, M. H. Shih, Y. C. Yang, and H. C. Kuo: Appl. Phys. Lett. **96** (2010) 151115.